Supplementary Information

A van der Waals porous crystal featuring conformational flexibility and permanent porosity for ultrafast water release

Kentaro Maejima,[1] Heishun Zen,[2] Hiroyasu Sato,[3] Eiji Nishibori,[4] Tomoya Enjou,[5] Youhei Takeda,[5] Satoshi Minakata,[5] Eri Hisamura,[6] Ken Albrecht,[6] Yuka Ikemoto,[7] Irene Badía-Domínguez,[8] Juan Sánchez-Rincón,[8] M. Carmen Ruiz Delgado,[8] Yohei Yamamoto,[1, †, *] and Hiroshi Yamagishi[1, †, *]

[1] Department of Materials Science, Institute of Pure and Applied Sciences, University of Tsukuba, 1-1-1 Tennodai, Tsukuba, Ibaraki 305-8573, Japan.

[2] Institute of Advanced Energy, Kyoto University, Gokasho, Uji, Kyoto 611-0011, Japan.

[3] Rigaku Corporation, 12-9-3 Matsubara, Akishima, Tokyo 196-8666, Japan.

[4] Department of Physics, Institute of Pure and Applied Sciences, University of Tsukuba, 1-1-1 Tennodai, Tsukuba, Ibaraki 305-8573, Japan.

[5] Department of Applied Chemistry, Graduate School of Engineering, Osaka University, 2-1 Yamadaoka, Suita, Osaka 565-0871, Japan.

[6] Institute for Materials Chemistry and Engineering, Kyushu University, 6-1 Kasuga-koen, Fukuoka 816-8580, Japan.

[7] Japan Synchrotron Radiation Research Institute (JASRI) SPring-8, 1-1-1 Koto, Sayo, Hyogo, 679-5198, Japan.

[8] Department of Physical Chemistry, University of Malaga, Campus de Teatinos s/n, 29071, Malaga, Spain.

[†] These authors jointly supervised this work

*e-mail: yamagishi.hiroshi.ff@u.tsukuba.ac.jp (H.Y.), yamamoto@ims.tsukuba.ac.jp (Y.Y.)

Supplementary Figures and Tables

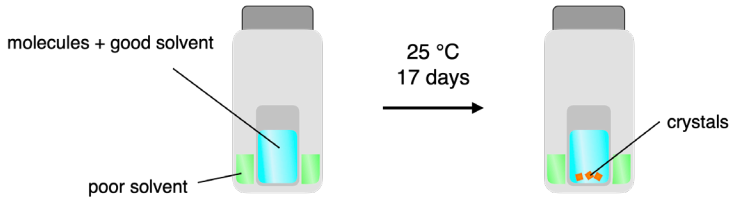

Figure S1. Schematic illustration of the crystallization.

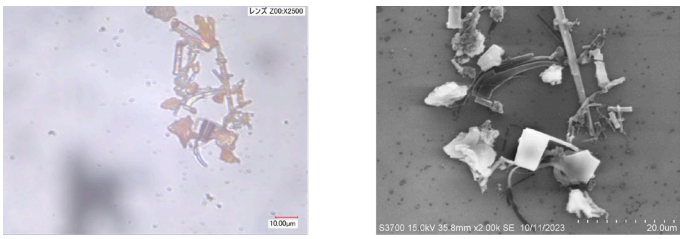

Figure S2. Optical microscope (OM) and scanning electron microscope (SEM) images of the crystalline grains of **VPC-1**.

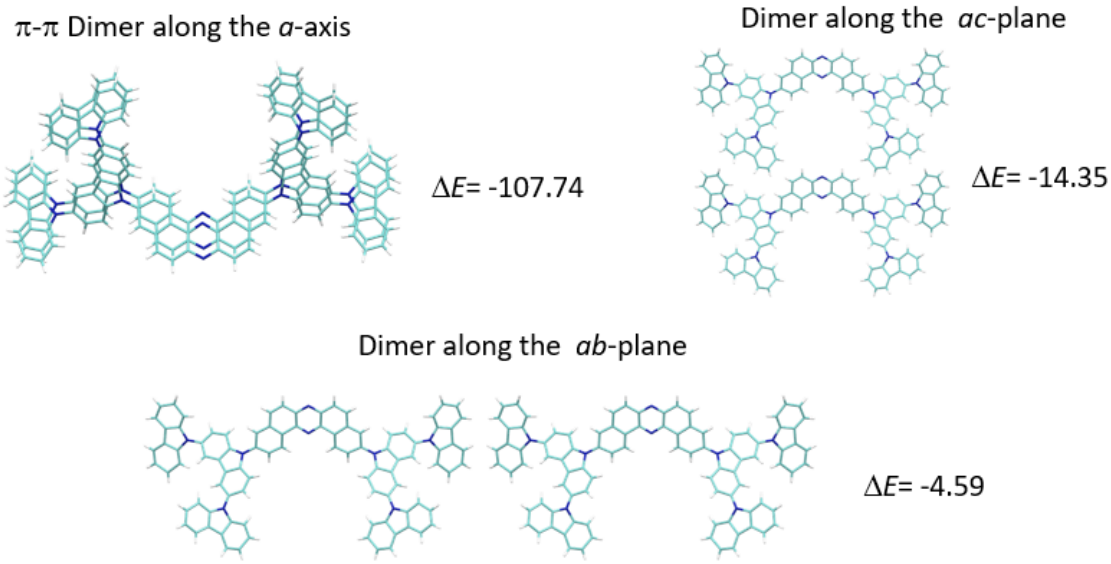

Figure S3. Interaction energies, ΔE (kcal mol^{-1}), for dimers along various crystal directions extracted from the crystal packing of **VPC-1** under vacuum, calculated at the ωB97XD/6-31G** level of theory.

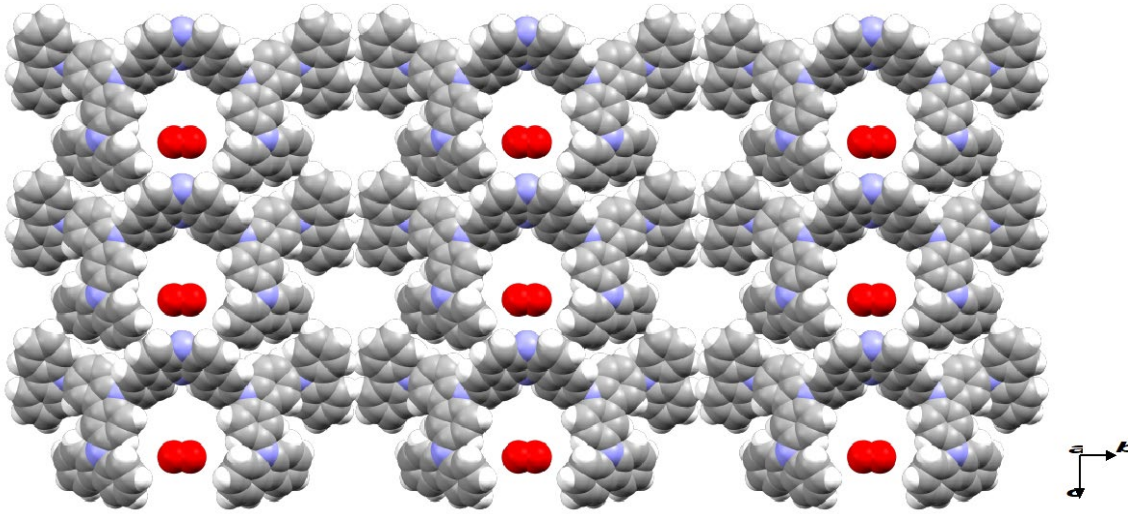

Figure S4. Crystal packing diagram of **VPC-1** under 0 %RH obtained with Rietveld refinement.

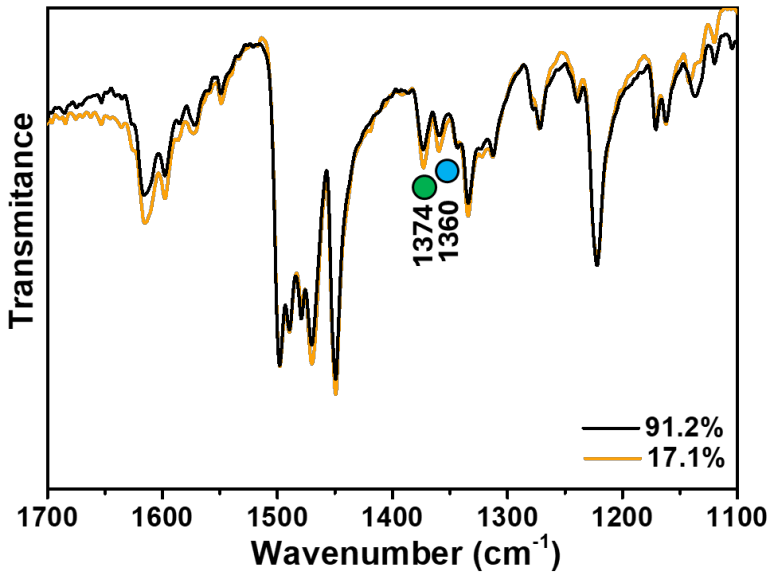

Figure S5. FTIR spectra of **VPC-1** on increasing the relative humidity at 25 °C. Data extracted from our previous work.[22] The dotted circles indicate the analogy with the theoretical normal modes shown in Figure S6.

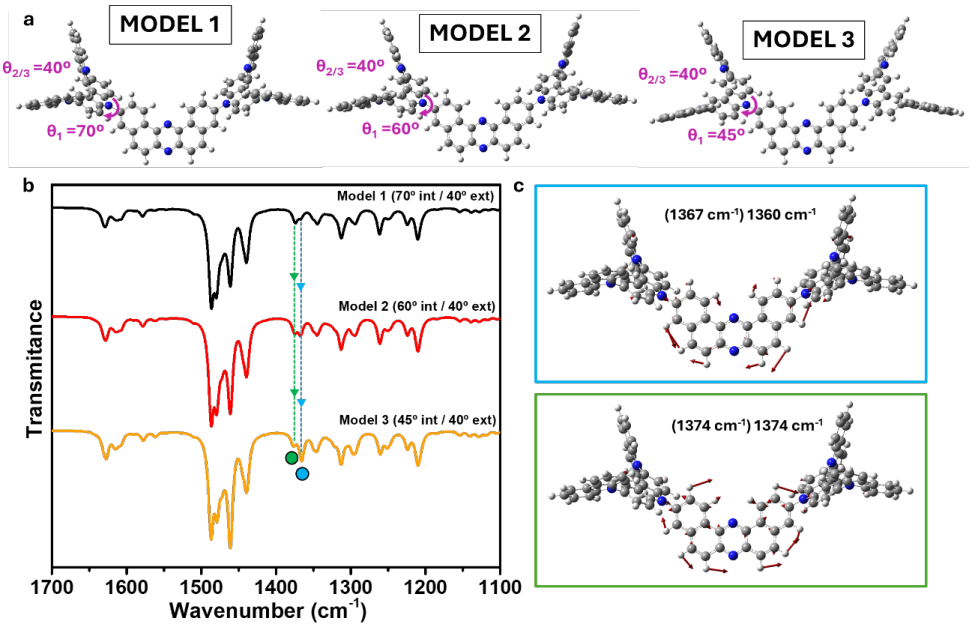

Figure S6. (a) A top-view of the three theoretical models proposed for **G2DBPHZ,** where the internal Cz dihedral angles (θ_1) are twisted 70° (model 1), 60° (model 2), 45° (model 3) whereas the external dihedral angles (θ_2 and θ_3) are kept fixed at 40°. (b) Theoretical IR spectra (CAM-B3LYP/6-31G** level) of the three models. (c) Eigenvectors associated to the infrared bands that are most affected by the relative humidity. The measured and theoretical (in parentheses) wavenumbers are also shown.

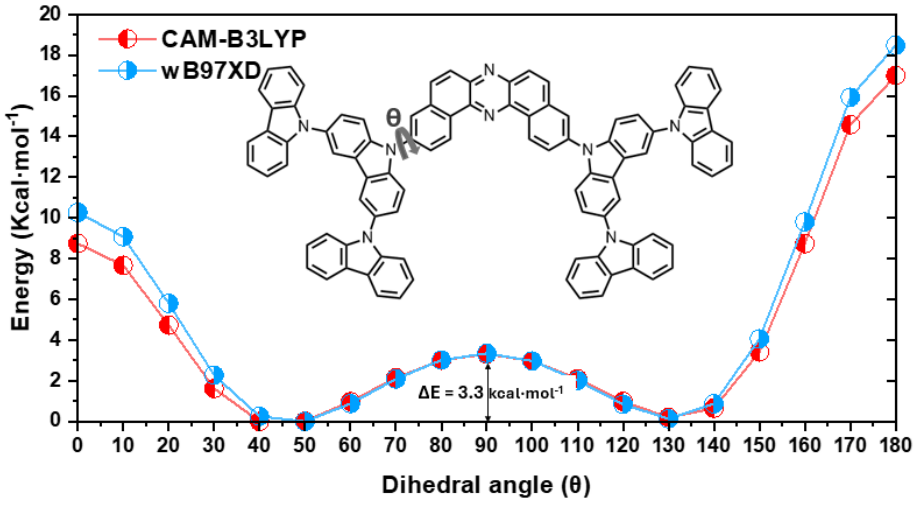

Figure S7. Rigid potential energy surface scan of **G2DBPHZ** as a function of the inter-ring dihedral angle (θ) between central DBPHZ spacer and the adjacent carbazole unit, calculated at the CAM-B3LYP/6-31G** and ωB97XD/6-31G** level of theory, respectively.

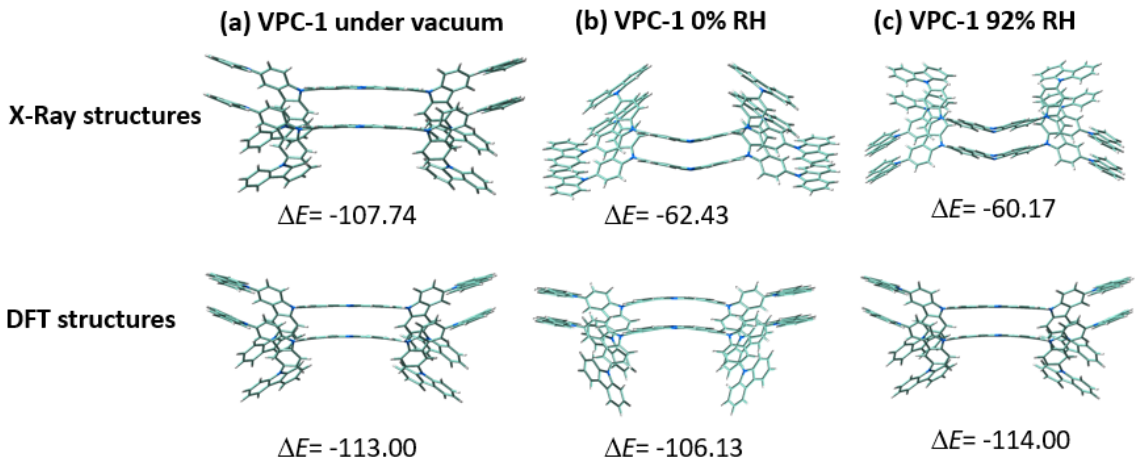

Figure S8. Interaction energies, Δ*E* (kcal mol-1), for π-π dimers extracted from crystal X-ray data (upper part) and reoptimized at the ωB97XD/6-31G** level of theory (lower part) for **VPC-1** under vacuum (a), under 0 %RH (b) and under 92 %RH (c).

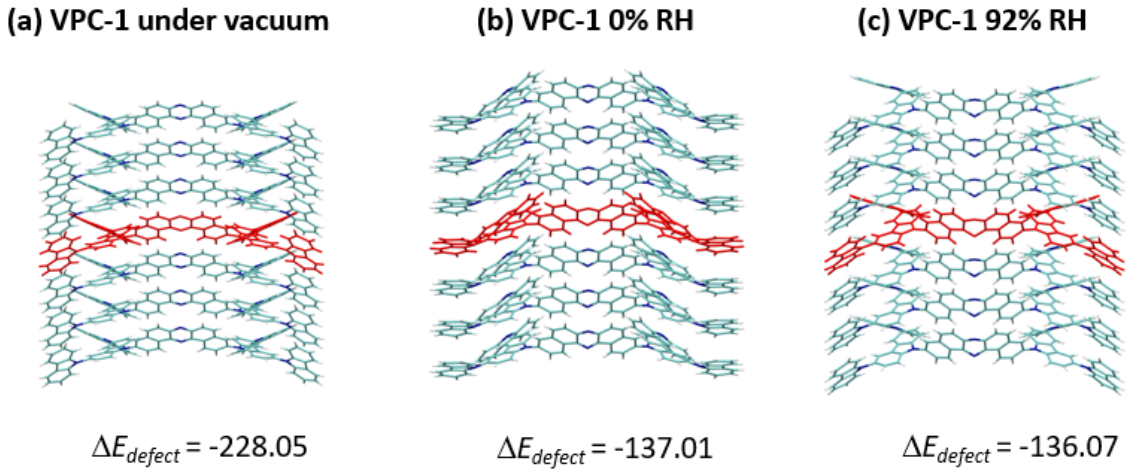

Figure S9. Interaction energies, Δ*E*defect (kcal mol^{-1}), for seven π-π stacked molecules extracted from the crystal packing of **VPC-1** under vacuum (a), under 0 %RH (b) and under 92 %RH (c). The defect energies has been evaluated as follows: Δ*E*defect = *E*(7 stacked molecules) - [*E*(7 stacked molecules – central molecule) + *E*(central molecule)].

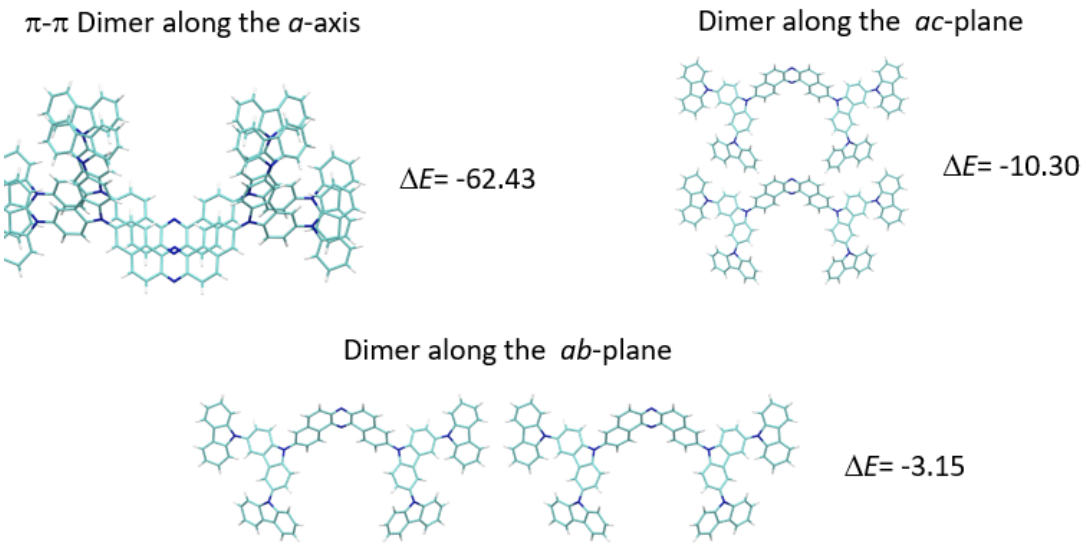

Figure S10. Interaction energies, ΔE (kcal mol^{-1}), for dimers along various crystal directions extracted from the crystal packing of **VPC-1** under 0 %RH, calculated at the ωB97XD/6-31G** level of theory.

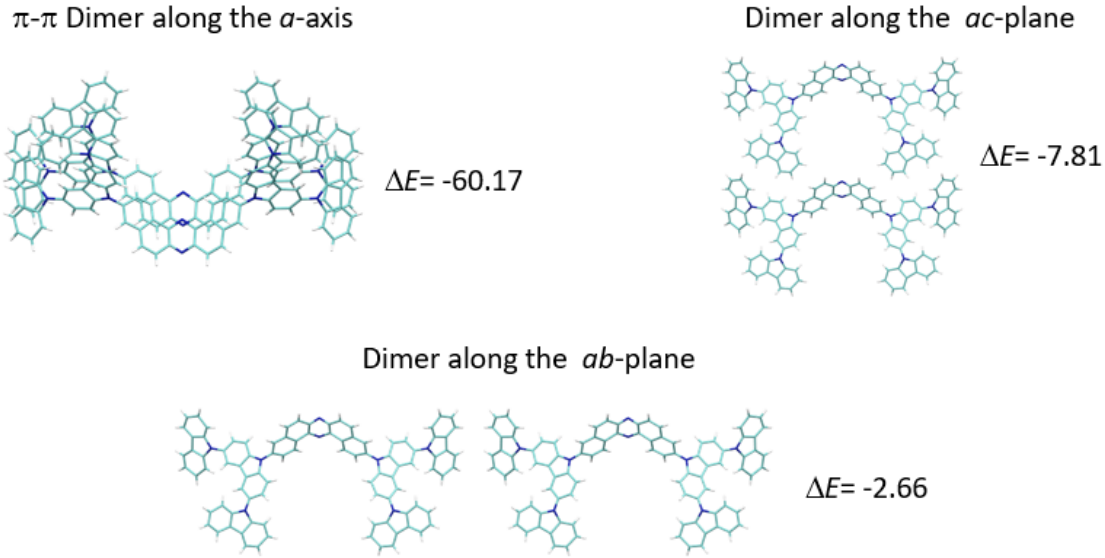

Figure S11. Interaction energies, ΔE (kcal mol^{-1}), for dimers along various crystal directions extracted from the crystal packing of **VPC-1** under 92 %RH, calculated at the ωB97XD/6-31G** level of theory.

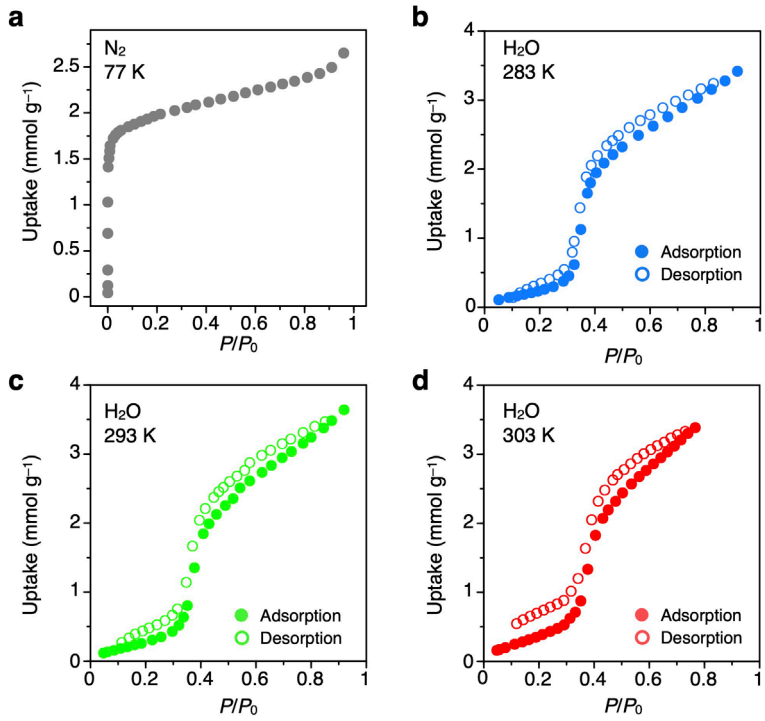

Figure S12. N_2 (a) and H_2O (b–d) isotherms of **VPC-1** measured at 77, 283,293, and 303 K, respectively. The data is reproduced from a reference without any modifications.[22]

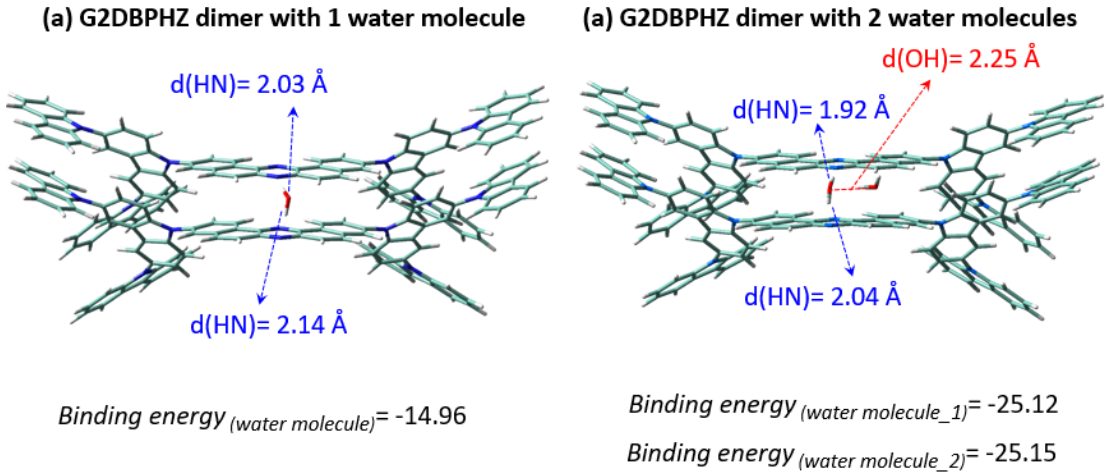

Figure S13. DFT-optimized geometries of a **G2DBPHZ** dimer with a H_2O molecule (a) and two H_2O molecules (b), calculated at the ωB97XD/6-31G** level of theory. The binding energies of the H_2O molecules (in kcal mol^{-1}) and the hydrogen bond distances formed between the H_2O molecules and with the N atoms of the DBPHZ core.

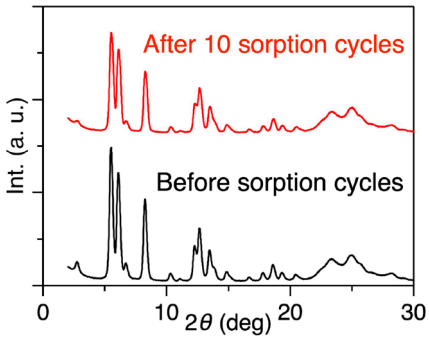

Figure S14. PXRD profiles of VPC-1 before (black curve) and after (red curve) 10 cycles of H_2O adsorption and desorption.

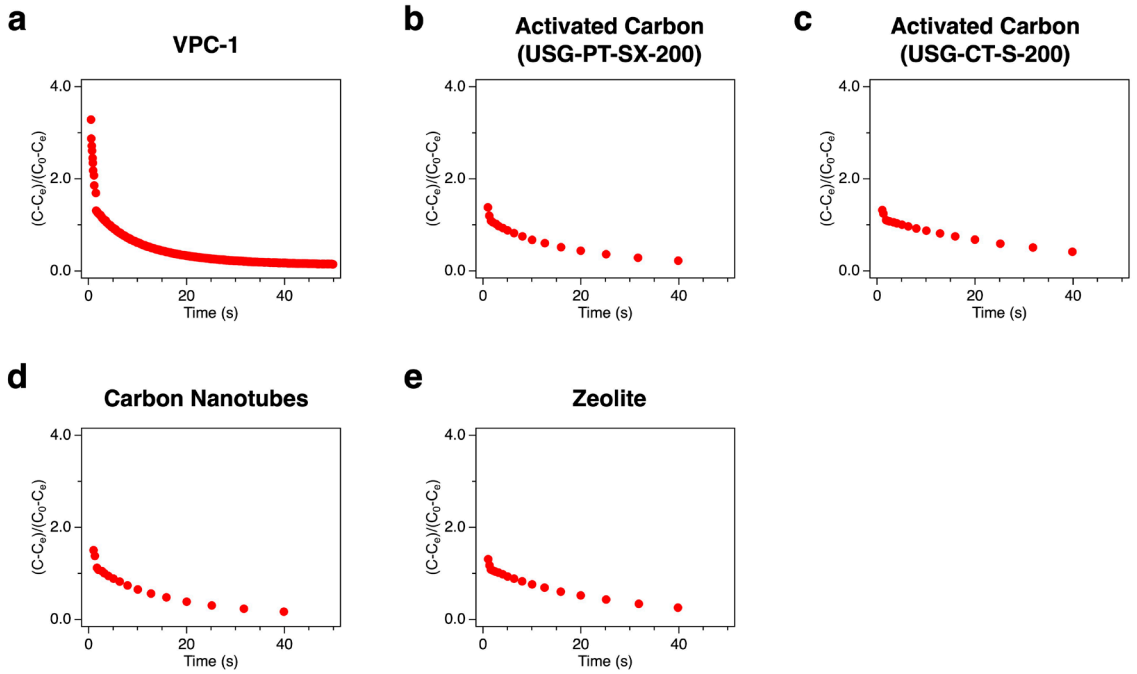

Figure S15. Time-course profile of $(C–C_e) / (C_0 – C_e)$ at 25 °C when introducing H_2O vapor to **VPC-1** (a), activated carbon for common gas (UES Co., Ltd., USG-PT-SX-200) (b), activated carbon for neutral gas (UES Co., Ltd., USG-CT-S-200) (c), carbon nanotubes (d), and zeolite A-5 (e). C is the concentration of water vapor, C_0 is the concentration of water vapor at t = 0 s, and C_e is the concentration of water vapor at equilibrium.

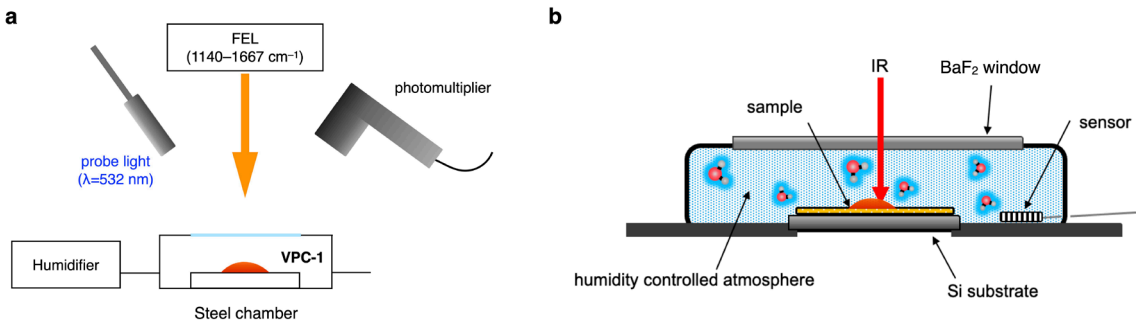

Figure S16. (a) Schematic illustration of the experimental setup for measuring diffuse reflectance of **VPC-1**, which was pumped with the infrared light generated from the free electron laser. (b) Detailed schematic illustration of the chamber.

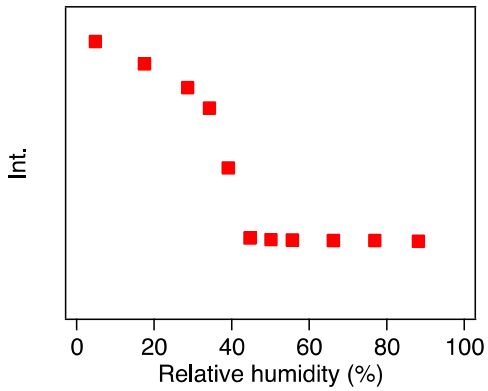

Figure S17. Plot of diffuse reflectance at 532 nm of **VPC-1** on experimental setup with IR irradiation.

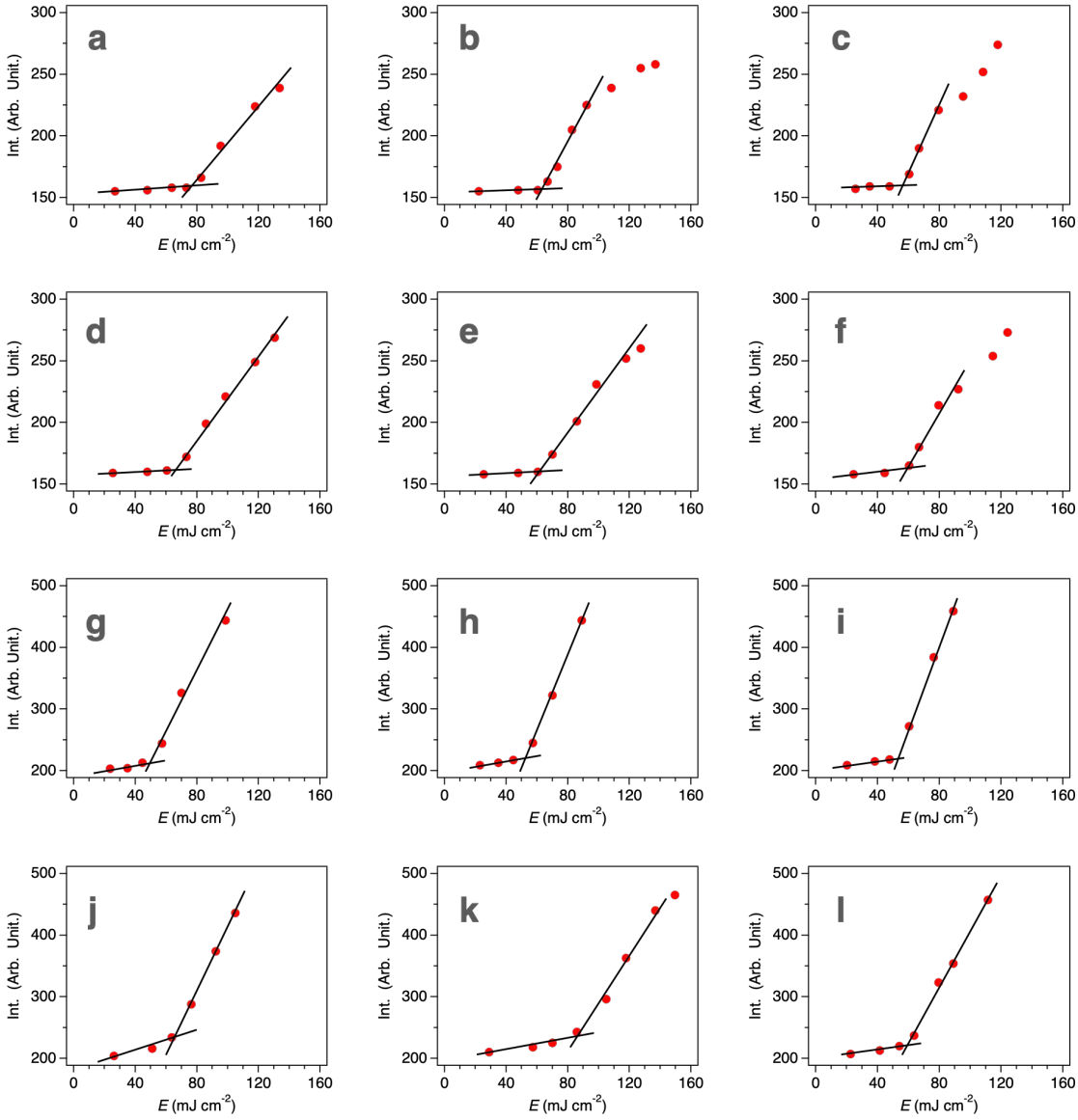

Figure S18. Plots of the diffuse reflectance of **VPC-1** as a function of *E* of the pump infrared light. The wavenumber of the pump laser was 1140 (a), 1170 (b), 1220 (c), 1273 (d), 1310 (e), 1342 (f), 1449 (g), 1470 (h), 1498 (i), 1598 (j), 1614 (k), and 1667 cm^{-1} (l).

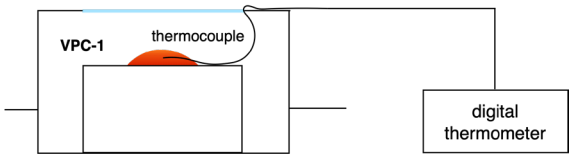

Figure S19. Schematic illustration of the setup for measuring the temperature of **VPC-1** during irradiation of the pump light. The thermocouple was set in the stack of **VPC-1**.

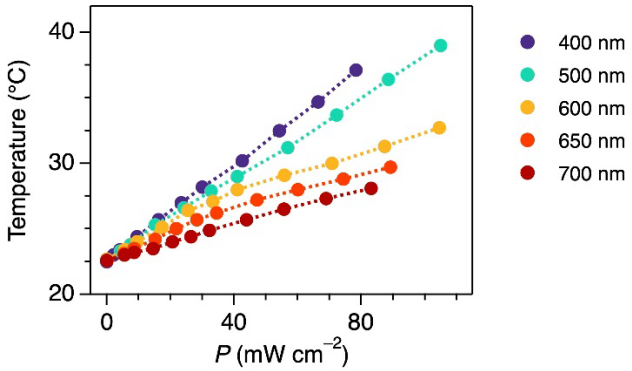

Figure S20. Plots of the temperature of **VPC-1** as a function of the P and λ of the pump light. The ambient temperature of **VPC-1** was 22.6 °C.

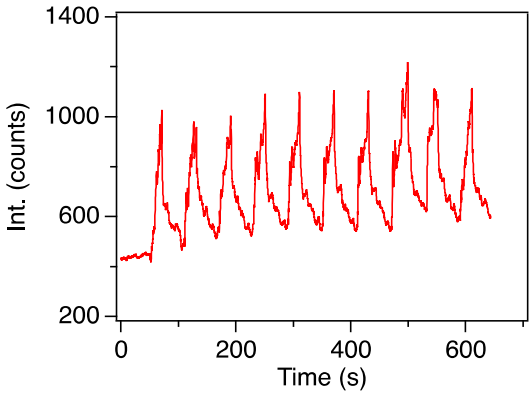

Figure S21. Time-course profile of diffuse reflectance of **VPC-1**. *P* of the pump light oscillated between 4.2 and 57 mW cm^{-2} repeatedly with an interval of 30 sec.

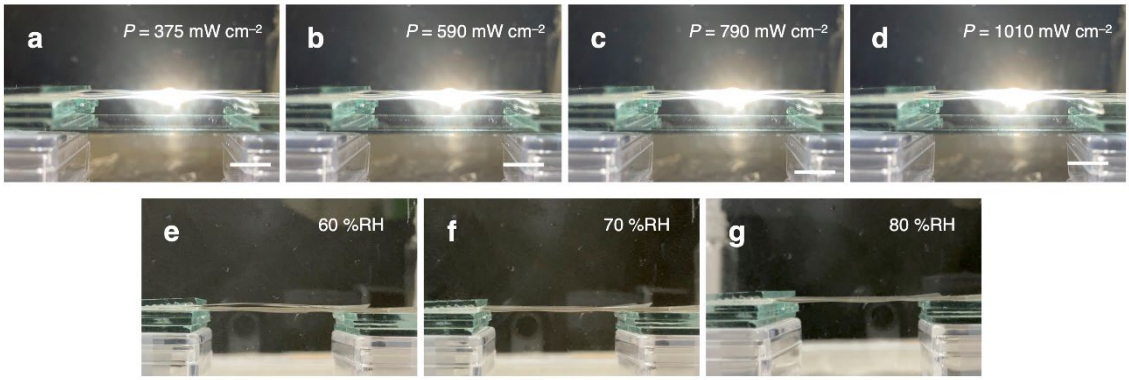

Figure S22. Photographs of the cellophane film put in the container without **VPC-1**. (a)–(d) The film was irradiated with a pump light (*P* = 375 (a), 590 (b), 790 (c), and 1010 (d) mW cm^{-2}). (e)–(g) The relative humidity in the container is set to be 60, 70, and 80 %RH. The films were not actuated in all the cases. Scale bars: 5 mm.

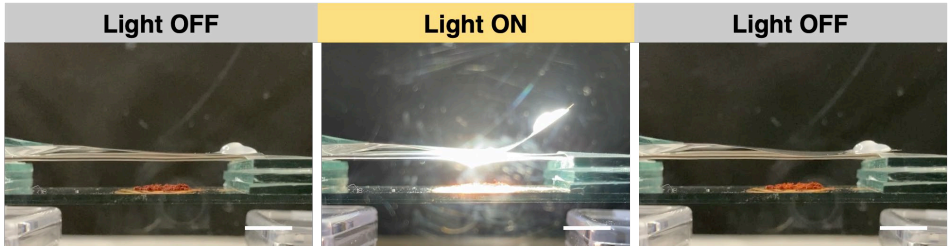

Figure S23. Photographs of a film actuated by the humidity from **VPC-1**. 20 mg weight silicon grease is loaded at the end of the film. Scale bars: 5 mm.

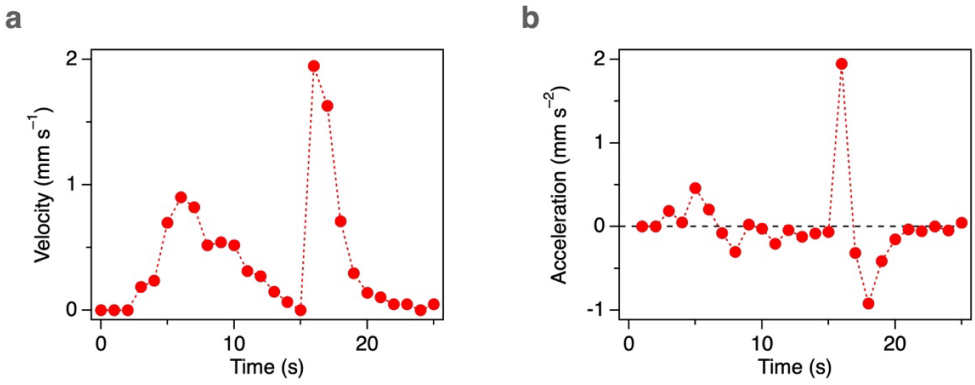

Figure S24. Time-course profile of velocity (a) and acceleration (b) of the film loaded with 20 mg silicon grease calculated based on the photographs.

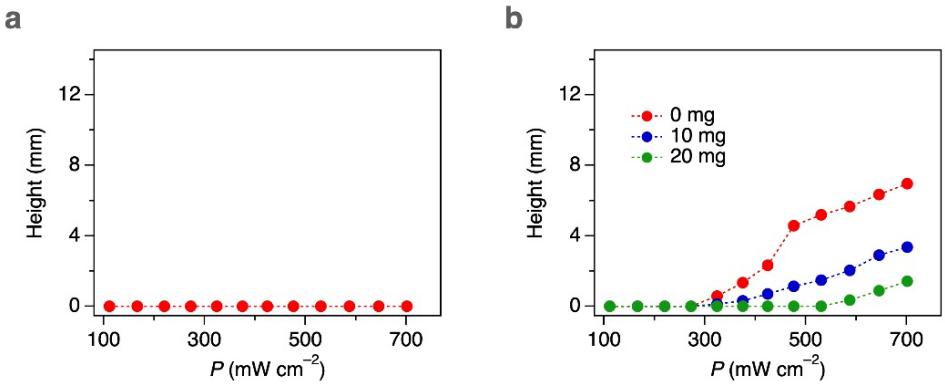

Figure S25. (a) Time-course profile of the height of the film edge when silica gel was put beneath the film instead of **VPC-1** and was irradiated with a white light as the pump. Silicon grease was not loaded on the film. (b) The amplitude of the film bending as a function of *P* when activated carbon was put beneath the film instead of **VPC-1** and was irradiated with a white light as the pump.

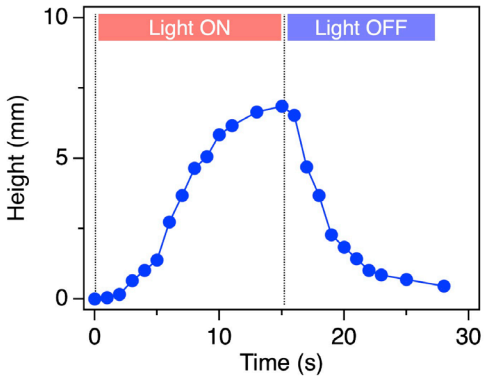

Figure S26. Time-course change in the height of film edge when irradiating activated carbon with the pump light.

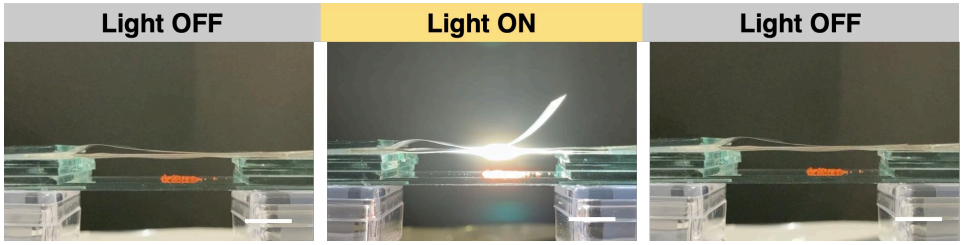

Figure S27. Photographs of the film actuated by **VPC-1** put in an open space. Scale bars: 5 mm.

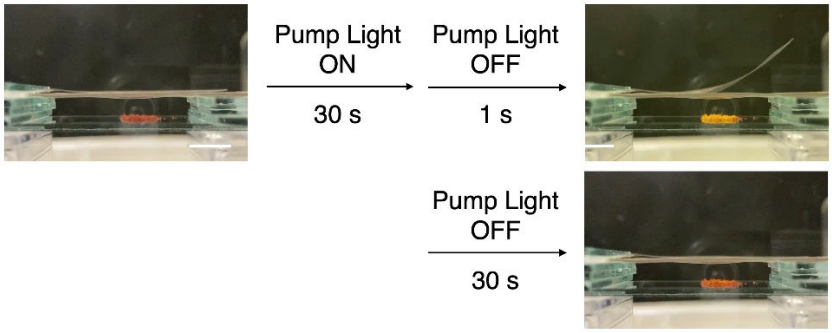

Figure S28. Photographs of **VPC-1** changing its color upon irradiation of the pump light. The color of **VPC-1** gradually turns back to red. Scale bars: 5 mm.

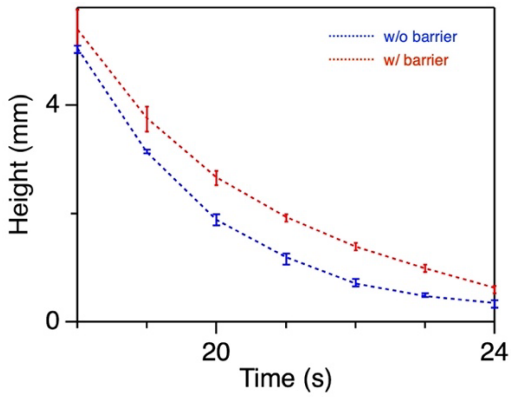

Figure S29. Magnified chart of Figure 4f with error bars (standard deviation, $n = 4$).

Table S1. Crystal structure information of **VPC-1** under vacuum.

Crystal data	
Formula	$C_{92}H_{54}N_8$
CCDC reference No.	2355950
Formula weight	1271.50
Temperature/K	293
Crystal system	monoclinic
Space group	*Cm*
a/Å	4.00(19)
b/Å	63.51(13)
c/Å	14.4(2)
α/°	90
β/°	94.6(5)
γ/°	90
Volume/Å^3	3642(181)
Z	2
ρ_{calc}g/cm^3	1.159
Crystal size/mm^3	0.002 × 0.0005 × 0.00001
Radiation	electron (λ = 0.0251)
2*Θ* range for data collection/°	0.208 to 1.796
Index ranges	-4 ≤ h ≤ 4, -77 ≤ k ≤ 77, -15 ≤ l ≤ 16
Reflections collected	7374
Independent reflections	5887 [R_{int} = 0.0676, R_{sigma} = 0.1816]
Data/restraints/parameters	5887/830/455
Goodness-of-fit on F^2	0.956
Final R indexes [I>=2σ (I)]	R_1 = 0.1210, wR_2 = 0.3067
Final R indexes [all data]	R_1 = 0.1813, wR_2 = 0.3598
Largest diff. peak/hole / *e* Å^{-3}	0.20/-0.15

Table S2. Crystal structure information of **VPC-1** under atmosphere at 0 %RH and 92 %RH.

Crystal data		
Humidity (%RH)	92	0
Chemical formula	$C_{46}H_{27}N_4 \cdot O$	$C_{46}H_{27}N_4 \cdot 4(O)$
M_r	651.72	699.72
Crystal system, space group	Monoclinic, *Cm*	Monoclinic, *Cm*
Temperature (K)	300	300
a, *b*, *c* (Å)	4.0139 (7), 63.583 (5), 14.4147 (10)	3.9926(7), 63.674(5), 14.4007(10)
β (°)	94.02 (2)	93.93(2)
V (Å^3)	3669.81	3652.38
Z	2	2
Radiation type	Synchrotron, λ = 1.00000 Å	Synchrotron,, λ = 1.00000 Å
Refinement		
R, *R*wp, *RI*	0.032, 0.045, 0.077	0.024, 0.035, 0.085
No. of reflections	273	271